International Journal of Microwave and Wireless Technologies

cambridge.org/mrf

SAR and thermal distribution of pregnant woman and child inside elevator cabin

Ioanna Karatsi[1], Sofia Bakogianni[2] and Stavros Koulouridis[1]

[1]Electrical and Computer Engineering Department, University of Patras, Polytechnic School, Patras, Greece and [2]Biomedical Engineering Department, University of West Attica, Egaleo, Attica, Greece

Research Paper

Cite this article: Karatsi I, Bakogianni S, Koulouridis S (2023). SAR and thermal distribution of pregnant woman and child inside elevator cabin. *International Journal of Microwave and Wireless Technologies* **15**, 213–226. https://doi.org/10.1017/S1759078722000253

Received: 25 August 2021
Revised: 1 February 2022
Accepted: 3 February 2022
First published online: 29 March 2022

Key words:
Finite-difference time-domain (FDTD); realistic human body; pregnant woman model; Pennes equation; specific absorption rate (SAR); power absorption

Author for correspondence:
Ioanna Karatsi,
E-mail: ioannak@ece.upatras.gr

Abstract

A detailed dosimetry study of electromagnetic absorption and temperature rise under real scenarios is delivered when a mobile phone is used inside an elevator cabin. Numerically accurate human models of a 7th month pregnant woman and a 5-year-old female child are utilized as the exposed subjects. The female child acts as the phone user. The mobile phone is modeled in three talk positions (parallel, tilt, and cheek) operating at 1000 MHz and 1800 MHz. From the obtained numerical results for the specific absorption rate (SAR) and temperature rise induced by the mobile radiofrequency (RF) radiation, it is found that the child's RF exposure is significantly affected by the phone position and less affected by the relevant position of the human models. The exact opposite case applies for the pregnant woman model and its fetus. Almost all numerical investigations are carried out inside a metallic elevator cabin.

Introduction

At the beginning of the 21st century, wireless services are well established within several technological sectors. Microwave and RF electromagnetic (EM) technology can be found at medical, industry, military, and domestic devices since there is the need of wireless connectivity. The most common use is the support of wireless mobile communications. In the last few years, the mobile phone has become an integral part of everyday life for numerous people. The concern of the safe exposure of humans at RF electromagnetic waves has attracted the scientific community.

The development of mobile phone technology has led to a rich pool of research studies to determine potential hazards caused by its use. It has been found that the rate of energy absorption in head tissues depends on the tissue properties (the dielectric properties, the mass density, and the anatomy of the head) and the characteristics of the RF radiation source (power, frequency, and distance) [1–7].

Furthermore, several studies have addressed the relationship between the spatially averaged specific absorption rate (SAR) and the local temperature rise induced by an RF source. Examining the exposure of anatomically based human whole-body models on EM plane waves, Razmadze *et al.* [8] found that the SAR averaged over 10 g of mass (SAR_{10g}) outmatches the SAR over 1 g of mass ($SAR_{1\,g}$) providing the best representations of the related steady-state temperature rise.

The obtained results from Sabbah *et al.* [9, 10] confirm the importance of performing a thermal analysis along with the electromagnetic dosimetry. Further, the effect of localized SAR should be related to the temperature rise in the head for cellular mobile phones [10]. Wessapan *et al.* [11, 12] found that the temperature distributions in the human head induced by mobile phone radiation are not directly proportional to the SAR distribution. This probably occurs because of the tissue dielectric and thermal properties, the blood perfusion, and the penetration depth of the electromagnetic power. The correlation between peak spatially averaged SAR and peak temperature rise in the human head by cell phone antennas was quantified by Hirata *et al.* [13, 14].

An important issue to highlight is that nowadays children tend to obtain a mobile phone even younger than the past years. It is also observed that parents allow preschool children to use a cell phone. Therefore, the attention of the scientists has moved on determining the potential hazards provoked from the use of mobile phones at sensitive population groups such as pregnant women and children.

Applying simplified phantoms of the human head as layered lossy dielectric spheres, Koulouridis *et al.* [15] observed similar levels of absorbed power (P_{abs}) between adult and children head models. Under specific simulation scenarios, Beard *et al.* [16] indicated that a larger head model (adult) reached a higher peak SAR than a smaller head (child). Furthermore, Christ *et al.*l [17] assessed that there are no age-dependent changes of the peak spatial SAR when averaged over the entire head whereas Gosselin *et al.* [18] indicated that a correlation

CAMBRIDGE UNIVERSITY PRESS

between the maximum $SAR_{10\,g}$ and the age of the head model could not be established for similar thicknesses of the pinna. Yet, Fernandez-Rodriguez *et al.* [19] confirmed that the peak spatial SAR (psSAR) in a child's brain is higher than in the adult's brain.

In [20], two-child head models (6 and 11 years old) and one adult head model (34 years old) were utilized, and it was found that the SAR distributions in the human brain are age dependent. Specifically, there is deeper penetration of the absorbed SAR in the child's brain and SAR can be significantly higher in subregions [20]. It seems that the increase in power absorption from a mobile phone is inversely proportional to the child's age due to differences such as a lower thickness of pinna, skin, and skull of the younger child models. It is indicated that, in general, children are more vulnerable to electromagnetic radiation than adults [21–23].

Moreover, radio frequency radiation from radio terminals upon a pregnant woman and her fetus has drawn the scientific attention due to the increased possibility of placing a mobile phone close to the abdomen. Takei *et al.* [24] underlined that the positional relationship between a smartphone, the placenta, and the fetus is of considerable importance. Research studies on radiation from mobile phone [25], portable radio terminals [26] and magnetic resonance imaging (MRI) [27] coils indicate that the SAR in the fetus depends on the frequency; a factor that impacts the penetration depth. Chiaramello *et al.* [28] found that the level of exposure of a fetus at the third trimester of pregnancy was higher than the first. Also, the higher the frequency is, the lower value of SAR is calculated at the fetus.

To address the EM near-field exposure of an Ultra High Frequency – Radio Frequency Identification (UHF – RFID) reader in adults, pregnant women, and children, Fiocchi *et al.* [29] found out that the highest exposure values in terms of the peak spatial $SAR_{10\,g}$ were acquired in the pregnant women. Also, Fiocchi *et al.* [30] pointed out that, under several exposure scenarios of pregnant women at RFID readers, the highest increase in temperature for two different pregnant women models was exhibited in the scenario in the front of the pregnant abdomen and in the oblique direction with respect to the abdomen. The exposure of pregnant women at polarized plane waves [31, 32] and at electromagnetic wave radiation from a smartphone [24] has been investigated indicating that the gestational age of the pregnant-women models affected the fetus averaged SAR.

EM exposure within metallic environments is, also, a topic of great interest because of the multiple wave reflections occurring inside or near them. The averaged SAR values can be increased inside metallic enclosures compared to free space [33–35] and at the presence of metallic walls [36, 37]. Whole-body exposure assessment might be equally significant with the peak averaged SAR values in the head at fully and partially enclosed metallic elevator cabins [38, 39]. The peak SAR averaged over 10 g mass of tissue depends on the position of the passenger and the antenna location against the elevator walls [40, 41]. Further, the dosimetry values depend on the number of people inside metallic enclosures [35, 42]. The structure of the enclosure and its material are important in determining SAR, as well [40]. Furthermore, as the buildings are getting taller and taller (e.g., department stores and companies), the need of wireless communication inside the elevator cabins has become important. Technology is providing many solutions [43] so that a mobile phone can be efficiently used inside the elevators.

This paper examines the electromagnetic exposure and thermal safety of a 5-year-old child and a 7th months pregnant woman, along with the fetus, inside an elevator cabin at a real-life scenario exposure. The cell phone, which is a numerically realistic model device [44], is placed at three different talk positions: parallel, tilt and cheek based on the IEEE/IEC 62209–1528-2020 std and CENELECEN 62209 standards [45, 46]. Two operating mobile phone frequencies at 1000 and 1800 MHz are implemented. The numerical dosimetry simulations were carried out with the commercially available EM software SEMCAD-X [47].

Specific absorption rate (SAR) & limits

Restrictions on human exposure to time-varying electromagnetic fields are well-established based on possible health effects. The physical quantity applied to determine these constraints is the SAR which represents the level of absorption of electromagnetic power by the biological tissue per unit mass of tissue. The SAR values at any point inside the tissue can be calculated as:

$$SAR = \frac{\sigma |E|^2}{\rho} [W/kg] \tag{1}$$

where σ (Si/m) is the electrical conductivity, ρ (kg/m^3) is the mass density of tissue and **E** is the effective value of the induced electric field.

The whole-body SAR can be calculated as:

$$SAR_{WB} = \frac{P_{abs}}{m} [W/kg] \tag{2}$$

where $P_{abs}(W)$ is the absorbed power and m (kg) is the whole mass of the absorber.

Standards for safety levels, with respect to human exposure to radiofrequency electromagnetic fields, determine that the maximum allowed peak spatial average SAR over 10 g of tissue is 2.0 W/kg and Whole-Body averaged SAR is 0.08 W/kg [48, 49]. The above values are calculated for 6 minutes of exposure.

Bioheat equation

The steady-state temperature distribution using the standard Pennes bioheat equation [50] is calculated by:

$$\rho c \frac{\partial T}{\partial t} = \nabla \cdot (k \nabla T) + \rho Q + \rho S - \rho_b c_b \rho \omega (T - T_b) \tag{3}$$

where ρ (kg/m^3) is the density of the medium, c (J/kg·°C) is the specific heat, T (°C) is the tissue temperature, t (sec) is the time, k (W/m·°C) is the thermal conductivity of the tissue, Q (W/kg) is the metabolic heat generation rate, S (W/kg) is the SAR, ω (m^3/kg·s) is the blood perfusion rate, ρ_b (kg/m^3) is the mass density, c_b (J/kg·°C) is the specific heat capacity, and T_b (°C) is the temperature of blood [51].

The boundary conditions for the temperature distribution applied in this study are the following [30, 52]:

- Mixed boundary condition:

$$k \frac{\partial T_{incr}}{\partial n} + h T_{incr} = 0 \tag{4}$$

https://doi.org/10.1017/S1759078722000253 Published online by Cambridge University Press

where h is the heat transfer coefficient, T_{incr} is the increased temperature and n is the unitary vector to the surface of the interface. Mixed boundary conditions were applied at the interfaces of tissues with the air. Between the skin and the outside air h was set as $h_{skin-air} = 8\ \mathrm{W/(m^2{\cdot}K)}$ and between the cornea and the external air h was set as $h_{cornea-air} = 20\ \mathrm{W/(m^2{\cdot}K)}$ [51].

- Neumann boundary condition:

$$k\frac{\partial T_{incr}}{\partial n} = 0 \tag{5}$$

Neumann boundary condition was applied at the interface between the tissues and the air-filled cavities (internal air, bronchi lumen, esophagus lumen, pharynx, and trachea lumen).

- Dirichlet boundary condition:

$$T_{incr} = 0 \tag{6}$$

Dirichlet boundary condition was applied at the interface between blood (artery, veins, and umbilical cord) and every tissue perfused by blood (all the tissues except air tissues, maternal and fetal cerebrospinal fluid (CSF), maternal and fetal humor vitreous, amniotic fluid, teeth, stomach lumen, and small intestine lumen). In addition, the external (to the body) room temperature was set as $T_{external} = 24°C$, and the temperature of the human models was set as $T_{human} = 37°C$.

A nonuniform mesh for the grid was used for both electromagnetic and thermal simulations with a minimum grid resolution of 1 mm at the source and at some tissues of human models. The maximum grid resolution at the environment (free space air) was 30 mm for both frequencies tested. This was accomplished by taking different max steps at 1000 and 1800 MHz due to the different wavelength λ (at 1000 MHz free space $\lambda = 299.79$ mm and at 1800 MHz free space $\lambda = 166.67$ mm). The total finite-difference time-domain (FDTD) calculation space varied from 46 5456 Mcells to 116 345 Mcells, depending on the simulation scenario and the mobile phone operating frequency.

Models and method

The utilized human models are numerically accurate anatomical models of a 7th months pregnant woman (Pregnant II) and a 5-year-old female child (Roberta) from the virtual population (VP), based on MRI [53].

The numerical mobile phone model consists of five different materials including the casing, the screen, the metal, the antenna substrate and air and it was developed by the French ANR project Kidpocket [44]. The antenna is located at the bottom of the mobile phone and operates at 1000 MHz and at 1800 MHz. The positioning point is symmetrically chosen to the horizontal axis of the phone and 5 mm below the top edge of the phone (see Fig. 1). The S11 parameter at free space for both frequencies is shown at Figs 2(a) and 2(b). The mobile antenna is fed with a voltage source of 1 V amplitude, and its resistance is 50 Ohm. The reference power is set to 1 W at both 1000 and 1800 MHz operating frequencies for comparison reasons and for compliance with the international research and bibliography.

According to the Greek Regulations for Buildings [54], buildings higher than 9 meters must be equipped with elevators that are able to serve people with disabilities and have a capacity for eight people. The minimum size of the recommended lift is 1.50 m × 1.70 m, and the corresponding dimensions of the cabin platform are 1.10 m × 1.40 m. An elevator cabin of dimensions $1.10 \times 1.40 \times 2.10\ \mathrm{m^3}$ and 10 mm thick walls was designed with an opening of 250 mm × 308 mm at the roof of the metallic enclosure (Fig. 3), based on the regulations for ventilation at elevators [55].

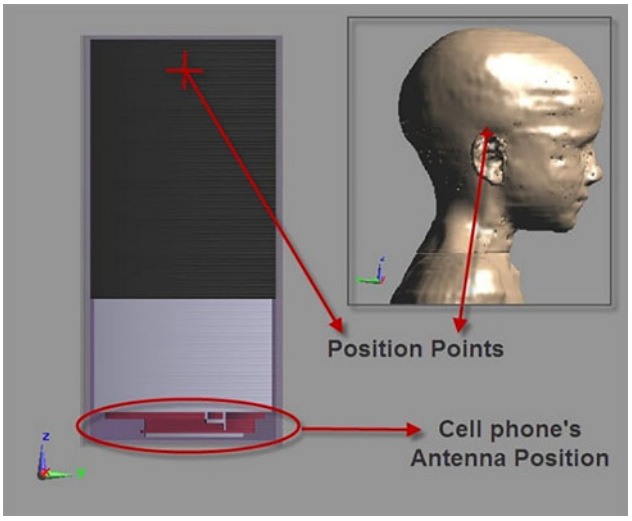

Fig. 1. Numerical mobile phone model (105 mm × 28.5 mm × 10 mm) and positioning points on phone and child human model (not in real scale).

The model of the pregnant woman (Pregnant II) is placed at the center of the metallic cabin and it is rotated around the vertical axis at eight different positions. The 5 years-old child Roberta is placed in the front part of the elevator cabin at a fixed distance, as shown in Fig. 4. The phone is placed on Roberta's right ear (left side at top view) at the side of the pregnant woman's abdomen. Further details on the positioning are provided below. As a result of the rotating Pregnant II model, the mobile phone is located at different positions in relation with the pregnant woman.

The two models were chosen so that the pregnant woman's abdomen is at the same height as the child's head. Specifically, the connection point between the Pregnant II and Roberta is fixed at the height of the mobile phone edge source, that coincides with the height of the pregnant woman's navel (Fig. 5).

The pregnant woman model is gradually rotated 45^{0} degrees around the z axis in eight different positions. The center of the pregnant woman model and the center of the lateral left side of its bounding box at the navel high define a circle of radius $r = 250.226$ mm and give the eight different positions as can be shown in Fig. 6. The distance of the two models is set to the minimum distance they can acquire, when the models' bounding boxes at the narrow side are connected (Fig. 6(b))

Figure 7 shows the positioning of the two models inside the elevator cabin and at free space, assuming a real case scenario with regular distances. The relevant positions of these models were chosen so that the phone is always located at the side of the pregnant woman, while the child, that is using the phone, is kept at a fixed location inside the cabin.

For all different configurations, the cell phone is placed in three different talk positions: (a) parallel (to z-axis), (b) tilt (with inclination to z-axis) and (c) cheek (with inclinations to

https://doi.org/10.1017/S1759078722000253 Published online by Cambridge University Press

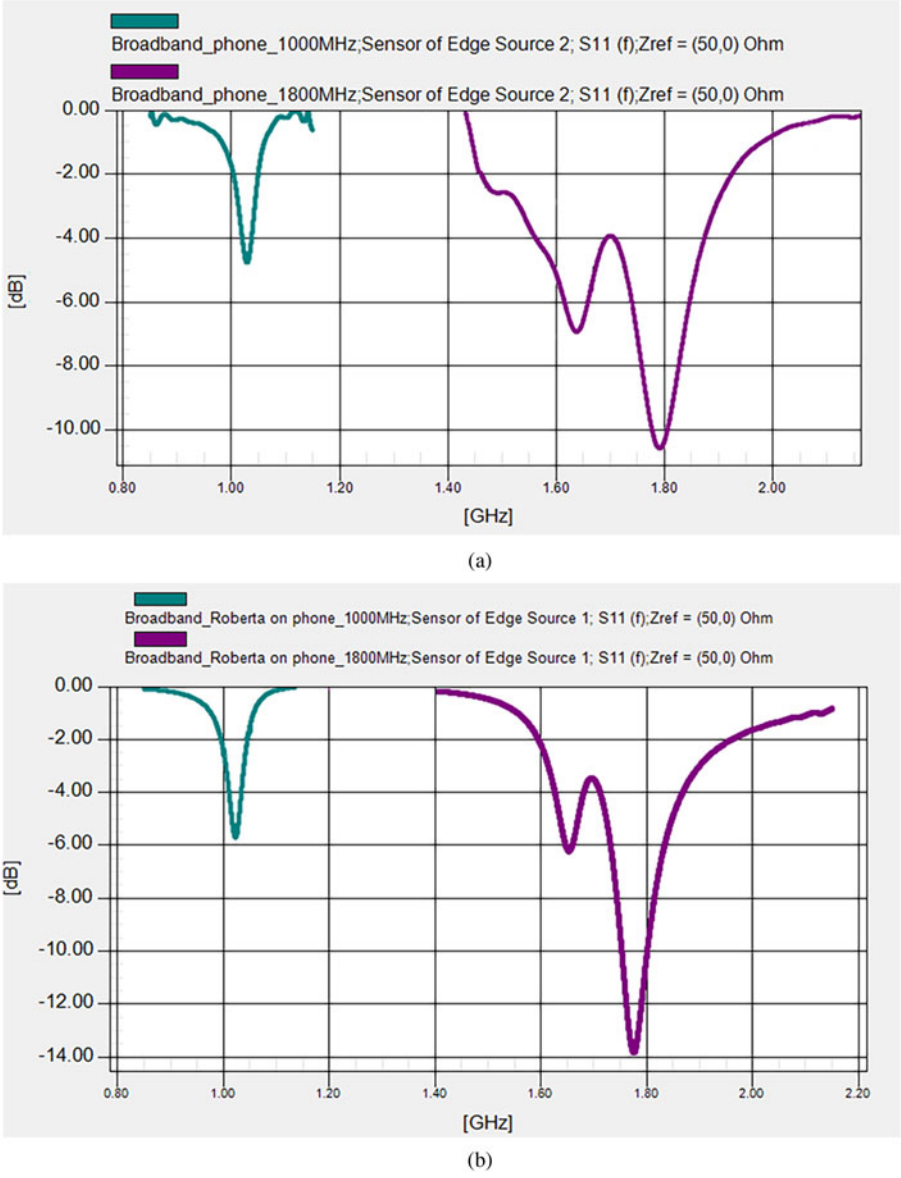

Fig. 2. S11 of the used mobile phone operating at 1000 MHz and at 1800 MHz: (a) in free space, and (b) with Roberta as the phone user at parallel talk position (see Fig. 8).

z-axis and x-axis), according to the IEEE 1528 std and CENELECEN 62209 standards [45, 46] (see Fig. 8).

Results and discussion

The obtained results are presented in this section. For the two utilized frequencies, the numerical data are successively given for each model. Averaged SAR over 10 g tissue mass, whole-body SAR and temperature increase are included within all graphic representations at 1000 and 1800 MHz and for the eight different model positions inside the metallic elevator cabin and at free space. First, the simulation results of the child's exposure are presented, then the respective data for the pregnant woman are provided, and, finally, the evaluation of the fetus exposure follows. The input power is set to $P_{in} = 1W$ for comparison reasons.

Mobile phone frequency at 1000 MHz

The $SAR_{10\,g}$ results and the temperature variations at 1000 MHz for the child mobile phone user, Roberta, are graphically presented in Fig. 9, while the whole-body SAR is provided in Fig. 10.

Based on the numerical data, the highest values of $SAR_{10\,g}$ are found at the cheek phone position for both free space and elevator configurations. The same is noticed for the induced temperature rise. The different relevant positions of the models produce small changes on the $SAR_{10\,g}$ values as well as on T_{max} values for the child phone user (Roberta). At free space, the maximum $SAR_{10\,g}$ value is calculated for human position 3 and is 5.161 W/Kg while inside the elevator cabin maximum $SAR_{10\,g}$ is 5.099 W/Kg for human position 2. The minimum $SAR_{10\,g}$ values at free space and inside the elevator cabin are found for parallel phone position and are 2.497 W/Kg, at human position 4 and 2.477 W/Kg, at human position 6 respectively.

Even though in our calculation, the local (point) maximum SAR value at free space is at the parallel position, in general, parallel and tilt positions exhibit lower $SAR_{10\,g}$ and T_{max} values for both free space and inside the elevator cabin as compared to cheek phone position. Tilt and parallel phone positions have both similar results, with small differences that depend on the different human models' relevant positions. Notably, $SAR_{10\,g}$ follows an increase of 5.79% from tilt to parallel phone position and

https://doi.org/10.1017/S1759078722000253 Published online by Cambridge University Press

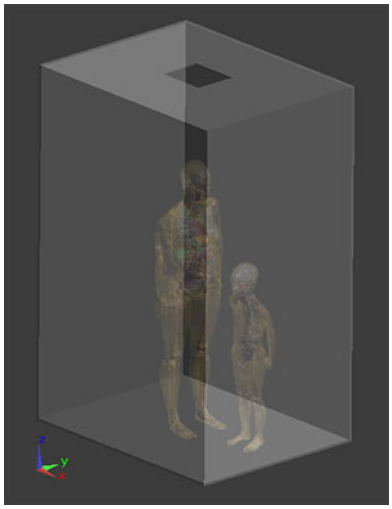

Fig. 3. The human models at position 1: inside the elevator metal cabin with a roof opening.

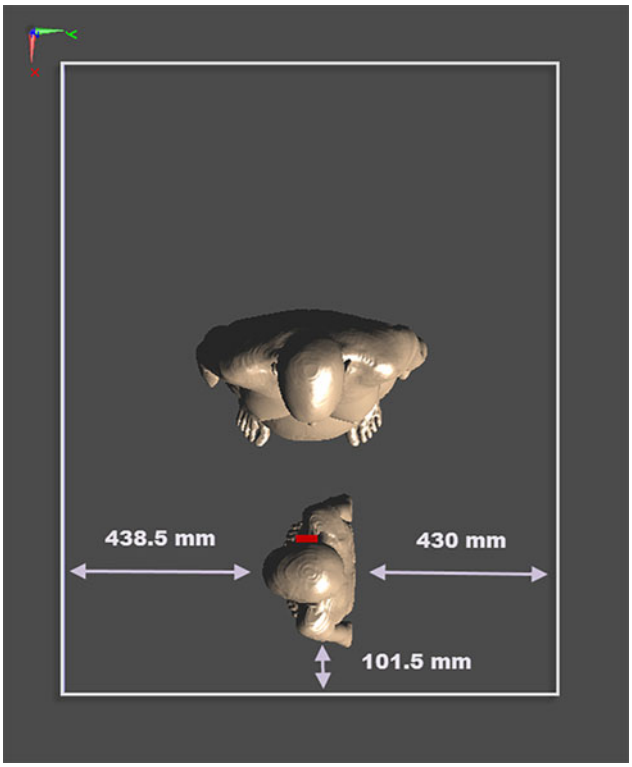

Fig. 4. Human models of the child and the pregnant woman inside the elevator cabin at position 1 (see Fig. 7); the cell phone is placed at Roberta's right ear.

33.46% from parallel to cheek phone position for Roberta at 1000 MHz. The presence of the elevator seems to cause an increase in almost all the values for both $SAR_{10\,g}$ and T_{max} and for the three different phone positions. In general, maximum temperature variations for Roberta are similar to $SAR_{10\,g}$ variations.

The whole-body SAR simulations conducted for Roberta present higher values compared to the corresponding ones in free space for the eight model relevant positions. In addition, the maximum SAR_{wb} is found at cheek phone position for both free space and elevator cabin cases and it is 0.043 W/Kg at human position 3

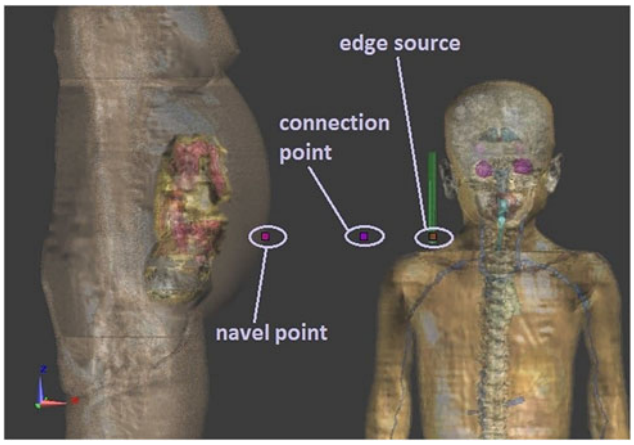

Fig. 5. Significant modeling points in the simulation environment at the same height at z axis: Pregnant woman navel, connection point between the human models, and cell phone edge source.

and 0.046 W/Kg at human position 8 respectively. The minimum SAR_{wb} value is calculated at parallel phone position for both free space and inside the elevator cabin and is 0.025 W/Kg at human position 4 and 0.032 W/Kg at human position 6 respectively. Cheek phone position at free space reveals higher values of SAR_{wb} than the tilt and parallel phone positions inside the elevator cabin. Still, free space tilt and parallel phone positions have lower values than the metallic cabin equivalents. Notably, the different relevant positions of human models create small differences at the SAR_{wb} values.

The $SAR_{10\,g}$ and the T_{max} of the 7th month pregnant woman (Pregnant II) at the 1000 MHz operating mobile phone frequency are presented in Fig. 11 while in Fig. 12 the whole-body SAR is provided.

For the pregnant woman model, the $SAR_{10\,g}$ as well as the temperature increase are affected both from the mobile phone position and the human models' relevant positions. T_{max} does not seem to be greatly affected by the elevator's presence, in contrast to $SAR_{10\,g}$ which seems to be more affected. The maximum values are found at parallel and tilt phone position at the human model position 3 (see Fig. 7). High values of $SAR_{10\,g}$ and T_{max} are also calculated for positions 6 and 7. The maximum $SAR_{10\,g}$ value is 0.406 W/Kg at parallel phone position at free space and 0.400 W/Kg at tilt phone position inside the elevator cabin. The minimum $SAR_{10\,g}$ value at 1000 MHz is 0.054 W/Kg at free space and 0.083 W/Kg inside the elevator cabin at human position 1 and cheek phone position for both cases. Maximum and minimum T_{max} measurements are well correlated, and they follow $SAR_{10\,g}$ findings.

The SAR_{wb} at 1000 MHz for Pregnant II exhibits the minimum and maximum values at the same talk phone positions as SAR_{10g}; the highest value can be found at the tilt phone position in the elevator cabin configuration, while the lowest value can be found at the cheek free space configuration. The maximum SAR_{wb} value is 0.00307 W/Kg at human position 5 at parallel phone position at free space and 0.00557 W/Kg at human position 6 at tilt phone position inside the elevator cabin. The minimum SAR_{wb} value at 1000 MHz is 0.0131 W/Kg at human position 8 at cheek phone position at free space and 0.0277 W/Kg at human position 8 at cheek phone position inside the elevator cabin. All elevator values are higher than the corresponding ones of free space. It is worth noting that the SAR_{wb} values are not affected by the human models' relevant positions while the $SAR_{10\,g}$ and T_{max}

https://doi.org/10.1017/S1759078722000253 Published online by Cambridge University Press

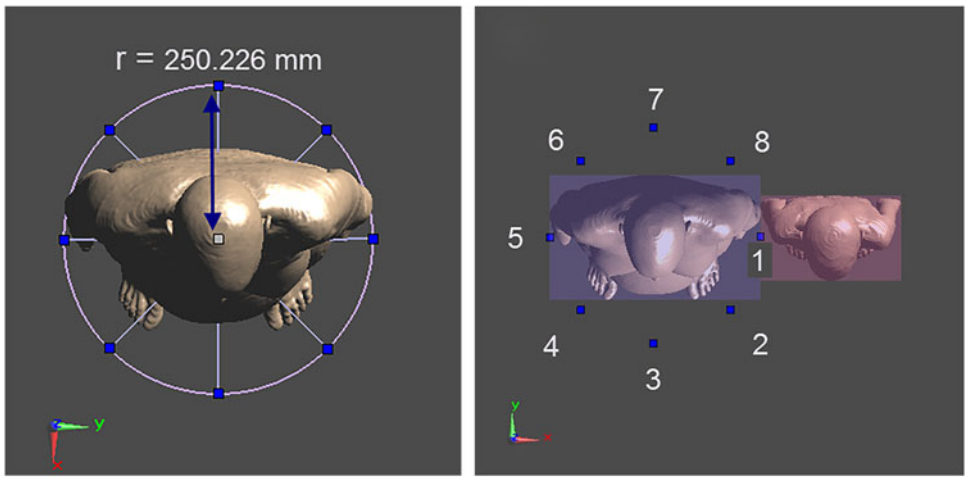

Fig. 6. (a) Pregnant woman position points, and (b) positions between human models with their bounding boxes shown.

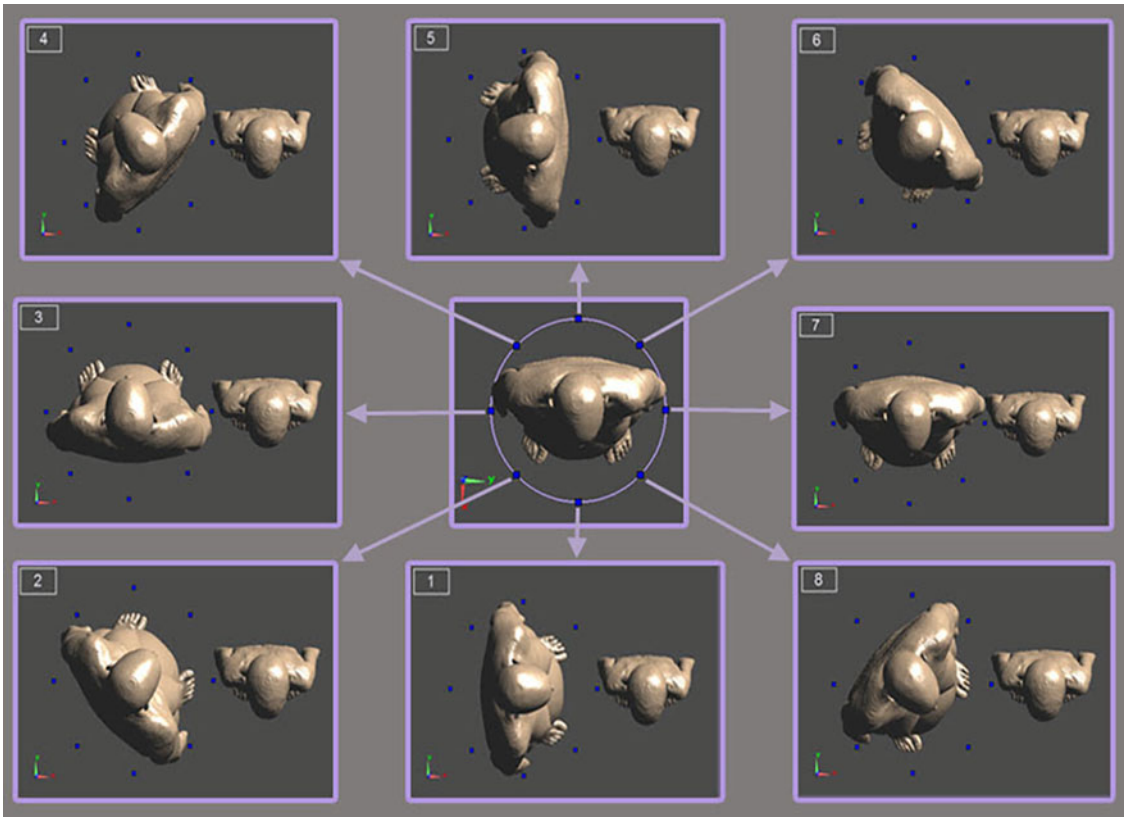

Fig. 7. The eight positions of child human model (Roberta) and pregnant woman model (Pregnant II).

values are greatly affected. SAR_{wb} variations are associated with phone talk position and the presence of the metallic cabin.

The $SAR_{10\,g}$ along with the T_{max} of the 7th month fetus for the operating mobile phone frequency of 1000 MHz are presented in Fig. 13, while in Fig. 14 the whole-fetus SAR is presented. For the fetus, the maximum $SAR_{10\,g}$ value at 1000 MHz is 0.0683 W/Kg at human position 8 at parallel phone position at free space and 0.0774 W/Kg at human position 7 at tilt phone position inside the elevator cabin. The next lower SAR10 g value is at tilt position at model position 1 inside the elevator cabin and is decreased by 11.7% from the first one. The minimum $SAR_{10\,g}$ value at 1000 MHz is 0.0001 W/Kg at four human positions at free space and 0.0029 W/Kg at human position 5 inside the elevator cabin. Minimum $SAR_{10\,g}$ is found at cheek phone positions.

The 7th month fetus' $SAR_{10\,g}$ and T_{max} distributions are different from those of the Pregnant woman. While the Pregnant model's maximum values are found at position 3 of the human models, the fetus' maximum values are found at positions 1, 7

https://doi.org/10.1017/S1759078722000253 Published online by Cambridge University Press

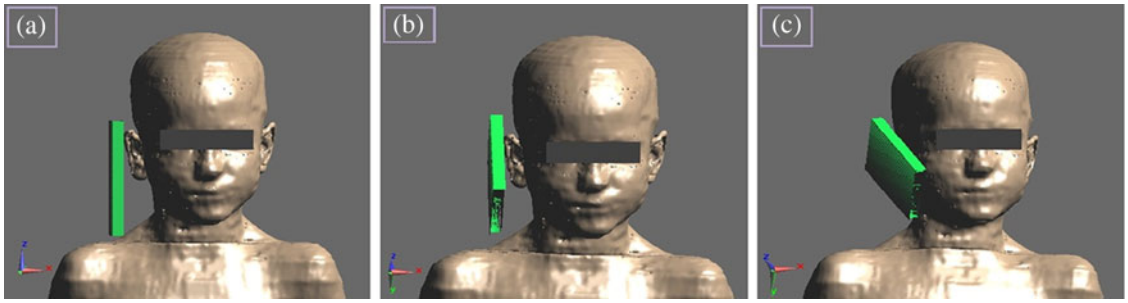

Fig. 8. Positions of mobile phone in relation with Roberta: (a) parallel position, (b) tilt position, and (c) cheek position.

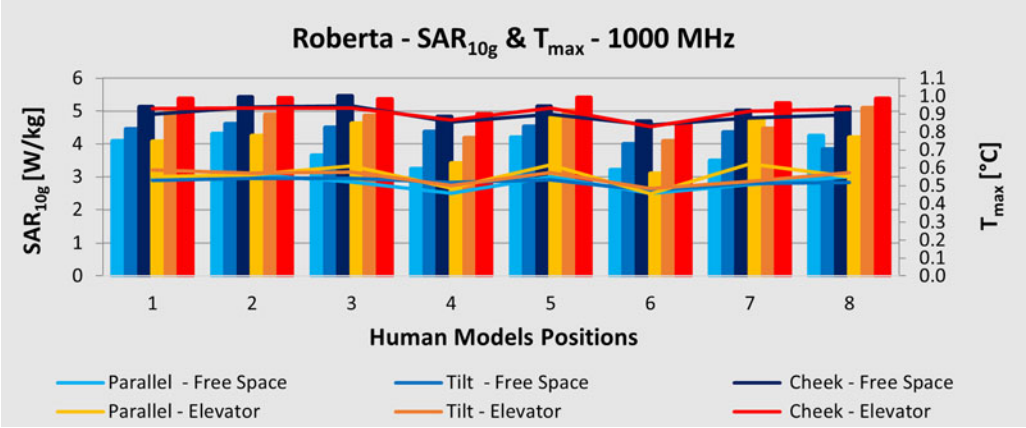

Fig. 9. Graphic representation of SAR10 g [W/kg] and Tmax rise [°C] values in child model Roberta at 1000 MHz and for 1 W output power of the mobile phone. Eight human model positions (see Fig. 7) and three mobile phone positioning inside the elevator cabin and at free space are evaluated. SAR values are represented by the line distributions while the bars correspond to the temperature values.

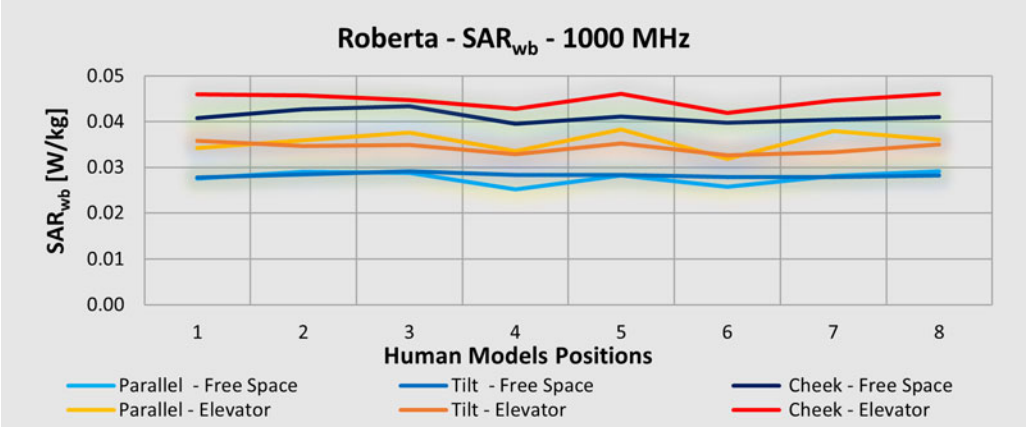

Fig. 10. Graphic representation of SAR whole-body (SARwb) [W/kg] in child model Roberta at 1000 MHz and for 1 W output power of the mobile phone. Eight human model positions (see Fig. 7) and three mobile phone positioning inside the elevator cabin and at free space are evaluated.

and 8; while position 3 of the model has very low T_{max} and $SAR_{10\,g}$ values for the fetus. At the tilt phone potion inside the elevator cabin the maximum measurements are found for both fetus and Pregnant II.

The whole-fetus SAR at 1000 MHz present almost the same distribution as the $SAR_{10\,g}$ and T_{max} for all the relevant configurations of the performed simulations. On the other hand, for the Pregnant II model the distributions of $SAR_{10\,g}$ are quite different from those of SAR_{wb}. The maximum SAR_{wb} value at 1000 MHz is 0.0088 W/Kg at free space and at human position 8, parallel phone position and 0.0101 W/Kg inside the elevator cabin at human position 8, tilt phone position. The minimum SAR_{wb} values, found at human position 4, cheek phone position, are 0.0001 W/Kg and 0.0006 W/Kg at free space and inside the elevator cabin respectively. Inside the elevator cabin there is an increase of 14.7% for SAR_{wb} maximum values. Inside the elevator, the SAR_{wb} values for all configurations are in general higher as compared to the corresponding free space ones.

https://doi.org/10.1017/S1759078722000253 Published online by Cambridge University Press

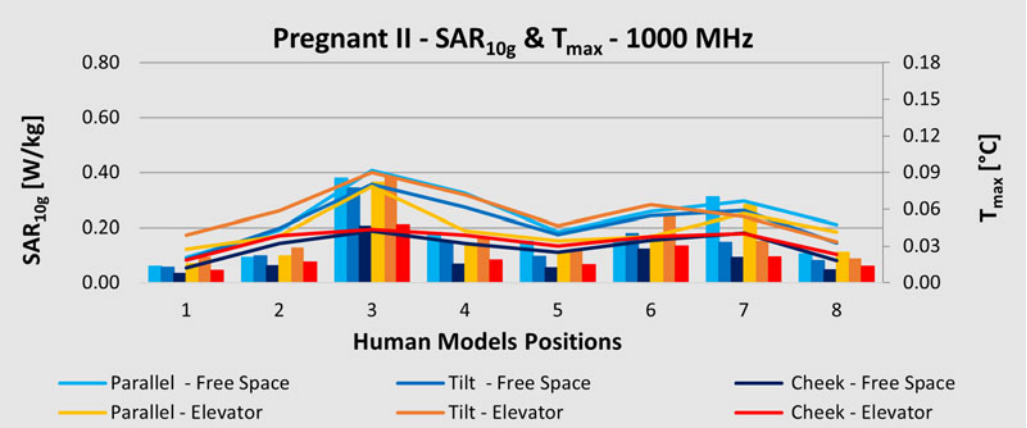

Fig. 11. Graphic representation of SAR10 g [W/kg] and Tmax rise [°C] values in 7th month pregnant model (Pregnant II) at 1000 MHz and for 1 W output power of the mobile phone. Eight human model positions (see Fig. 7) and three mobile phone positioning inside the elevator cabin and at free space are evaluated. SAR values are represented by the line distributions while the bars correspond to the temperature values.

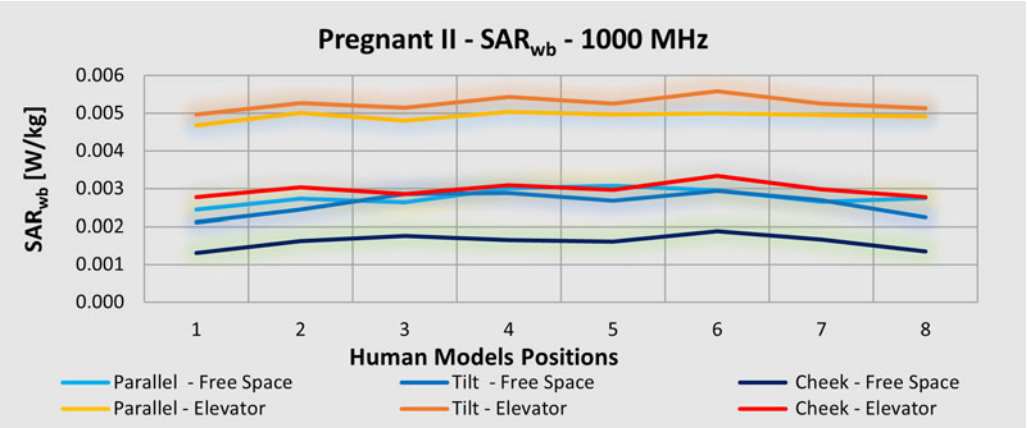

Fig. 12. Graphic representation of SAR whole-body (SARwb) [W/kg] in 7th month pregnant model (Pregnant II) at 1000 MHz and for 1 W output power of the mobile phone. Eight human model positions (see Fig. 7) and three mobile phone positioning inside the elevator cabin and at free space are evaluated.

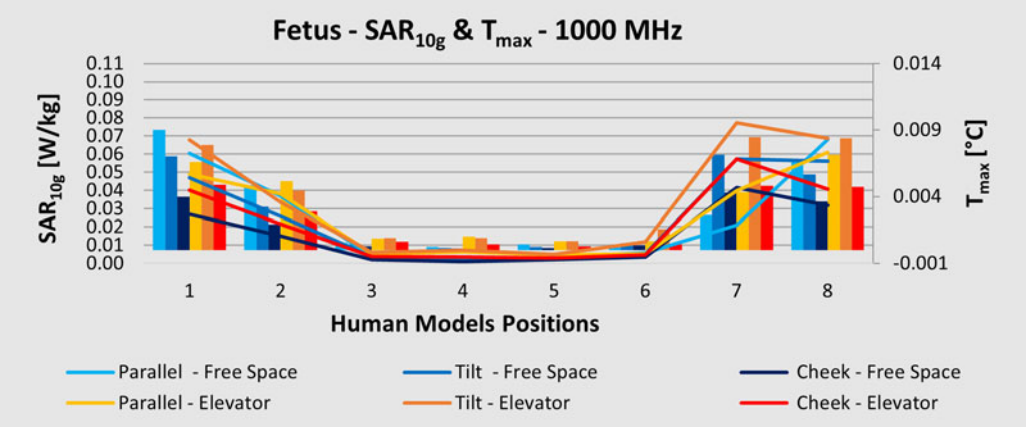

Fig. 13. Graphic representation of SAR10 g [W/kg] and Tmax rise [°C] values in 7th month model fetus at 1000 MHz and for 1 W output power of the mobile phone. Eight human model positions (see Fig. 7) and three mobile phone positioning inside the elevator cabin and at free space are evaluated. SAR values are represented by the line distributions while the bars correspond to the temperature values.

https://doi.org/10.1017/S1759078722000253 Published online by Cambridge University Press

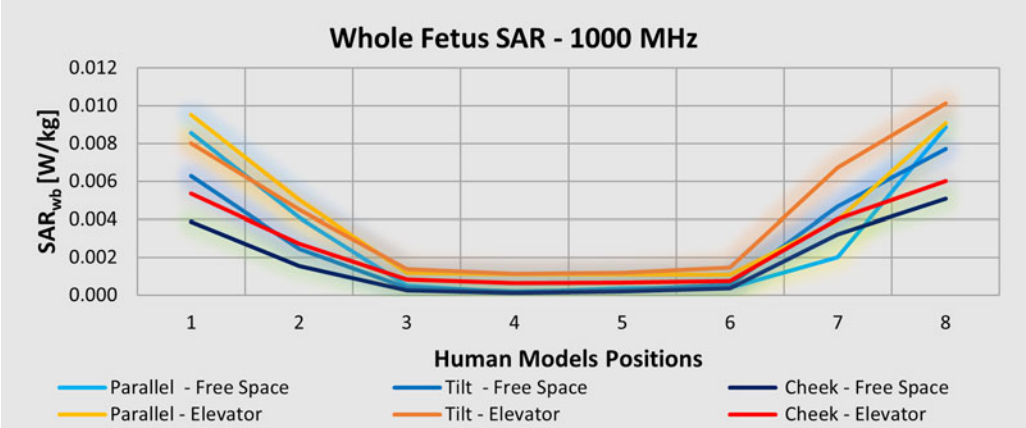

Fig. 14. Graphic representation of SAR whole-body (SAR-wb) [W/kg] in 7th month model fetus at 1000 MHz and for 1 W output power of the mobile phone. Eight human model positions (see Fig. 7) and three mobile phone positioning inside the elevator cabin and at free space are evaluated.

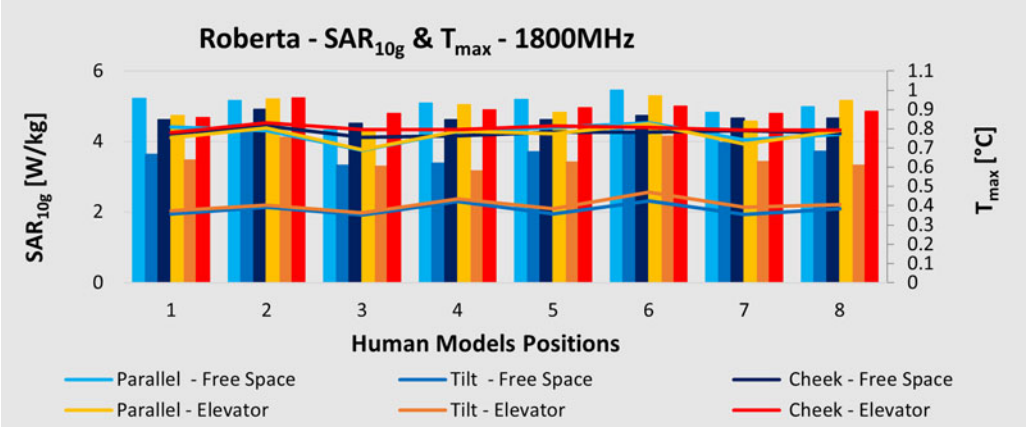

Fig. 15. Graphic representation of SAR10 g [W/kg] and Tmax rise [°C] values in child model Roberta at 1800 MHz and for 1 W output power of the mobile phone. Eight human model positions (see Fig. 7) and three mobile phone positioning inside the elevator cabin and at free space are evaluated. SAR values are represented by the line distributions while the bars correspond to the temperature values.

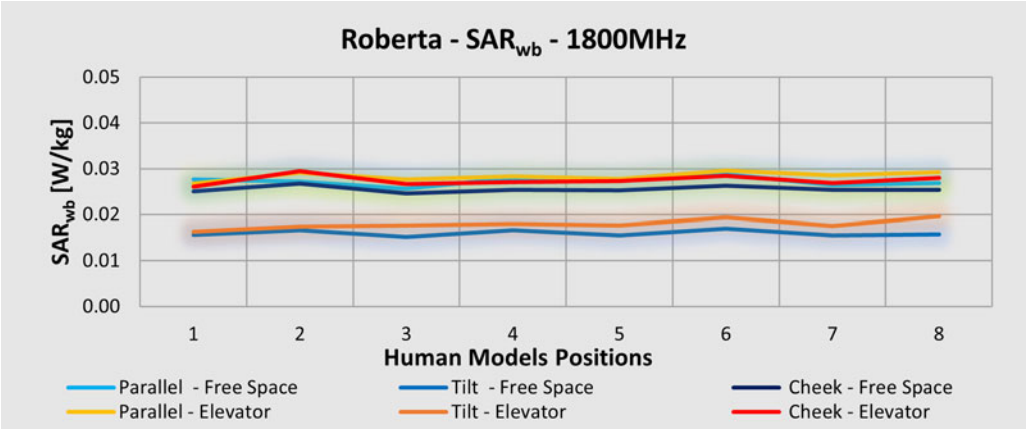

Fig. 16. Graphic representation of SAR whole-body (SARwb) [W/kg] in child model Roberta at 1800 MHz and for 1 W output power of the mobile phone. Eight human model positions (see Fig. 7) and three mobile phone positioning inside the elevator cabin and at free space are evaluated.

Mobile phone frequency at 1800 MHz

The $SAR_{10\,g}$ results and the temperature variations at 1800 MHz operating mobile frequency for the child phone user, Roberta, are graphically presented in Fig. 15, while in Fig. 16 the whole-body SAR is presented.

At 1800 MHz, the highest values of $SAR_{10\,g}$ and T_{max} for Roberta are found at the cheek and parallel phone positions respectively. Tilt phone position presents the lowest $SAR_{10\,g}$ values as well as the lowest temperature rise. The T_{max} values at the parallel position are slightly higher than the cheek phone

https://doi.org/10.1017/S1759078722000253 Published online by Cambridge University Press

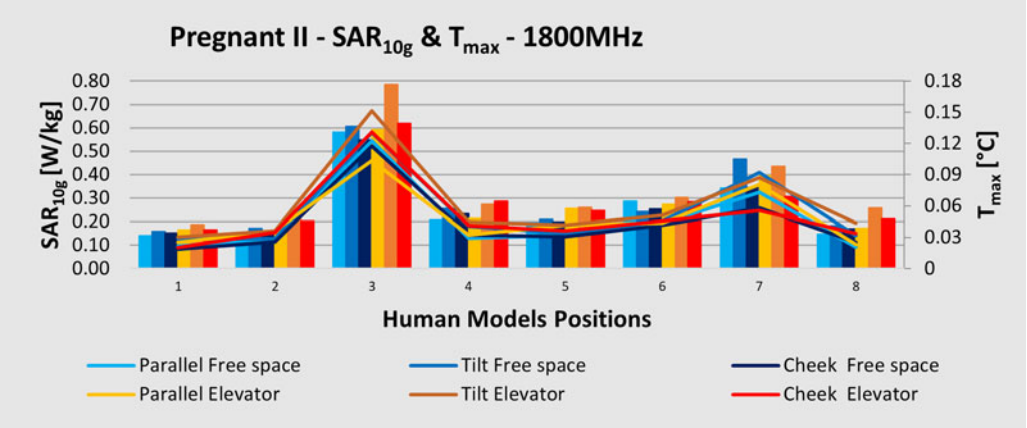

Fig. 17. Graphic representation of SAR10 g [W/kg] and Tmax rise [°C] values in 7th month pregnant model (Pregnant II) at 1800 MHz and for 1 W output power of the mobile phone. Eight human model positions (see Fig. 7) and three mobile phone positioning inside the elevator cabin and at free space are evaluated. SAR values are represented by the line distributions while the bars correspond to the temperature values.

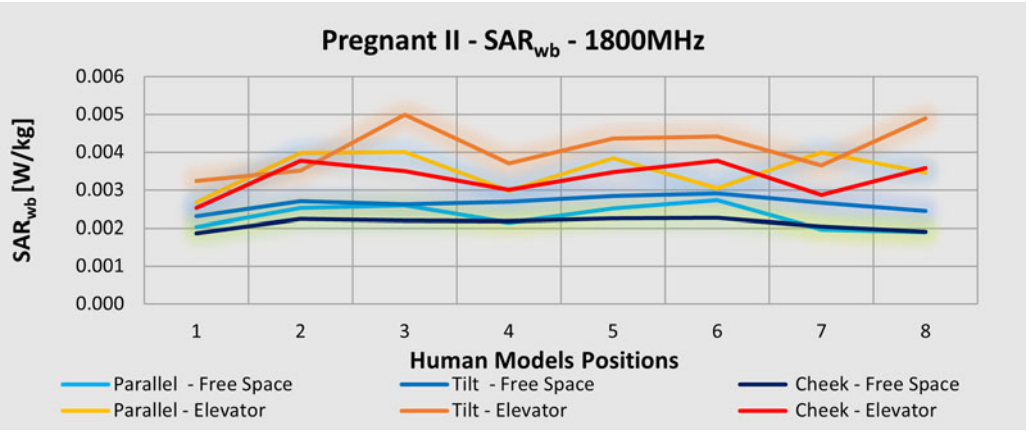

Fig. 18. Graphic representation of SAR whole-body (SARwb) [W/kg] in 7th month pregnant model (Pregnant II) at 1800 MHz and for 1 W output power of the mobile phone. Eight human model positions (see Fig. 7) and three mobile phone positioning inside the elevator cabin and at free space are evaluated.

positions at free space and inside the elevator cabin, as well. Further, $SAR_{10\,g}$ values are higher at the cheek position inside the metallic elevator cabin. Almost all calculated results inside the elevator cabin are slightly higher than the corresponding ones in free space, especially the $SAR_{10\,g}$ values.

The maximum $SAR_{10\,g}$ value at 1800 MHz is 4.523 W/Kg at human position 6 and parallel phone position at free space and 4.529 W/Kg at human position 2 and cheek phone position inside the elevator cabin. The minimum $SAR_{10\,g}$ values at 1800 MHz are 1.914 W/Kg at human position 3 and tilt phone position at free space and 1.972 W/Kg at human position 1 and tilt phone position inside the elevator cabin. $SAR_{10\,g}$ increases 48.81% from tilt to parallel phone position and 0.71% from parallel to cheek phone position for Roberta at 1800 MHz. In contrary to 1000 MHz, the highest values of T_{max} are found at the parallel phone position. Still, the maximum $SAR_{10\,g}$ values are similarly found at the cheek phone position. All $SAR_{10\,g}$ maximum values for 1000 MHz are found at ear skin at parallel and tilt position while at 1800 MHz the maximum values for these two phone positions are at ear cartilage. At cheek phone position for both 1000 and at 1800 MHz maximum values have been found at muscle tissue. The relevant positions of human models slightly affect the values of both T_{max} and $SAR_{10\,g}$ and for both operating frequencies.

While at 1000 MHz the whole-body SAR exhibits the maximum values at the cheek elevator phone position inside the metallic cabin, at 1800 MHz the SAR_{wb} has similar results for the parallel and cheek phone position at all models' relevant positions. The maximum SAR_{wb} value at 1800 MHz is 0.029 W/Kg at human position 3 at cheek phone position at free space and 0.030 W/Kg at human position 8 at cheek phone position inside the elevator cabin. The minimum SAR_{wb} value at 1800 MHz is 0.015 W/Kg at human position 4, parallel phone position at free space and 0.016 W/Kg at human position 6, parallel phone position inside the elevator cabin. Free space results present slightly lower values than the corresponding ones inside the metallic cabin. Tilt phone position at free space has the lowest SARwb values for Roberta. Generally, the SAR_{wb} for the child Roberta is higher at 1800 MHz than at 1000 MHz for all configurations.

The $SAR_{10\,g}$ and the T_{max} of the 7th month pregnant woman (Pregnant II) at the 1800 MHz operating mobile phone frequency are presented in Fig. 17 while in Fig. 18 the whole-body SAR is provided. For the pregnant human model, the maximum $SAR_{10\,g}$ and T_{max} values are found, similarly as for 1000 MHz case, at the human models position 3. The maximum $SAR_{10\,g}$ value is 0.606 W/Kg at free space and 0.786 W/Kg inside the elevator cabin, both at tilt phone position. At free space, the minimum

https://doi.org/10.1017/S1759078722000253 Published online by Cambridge University Press

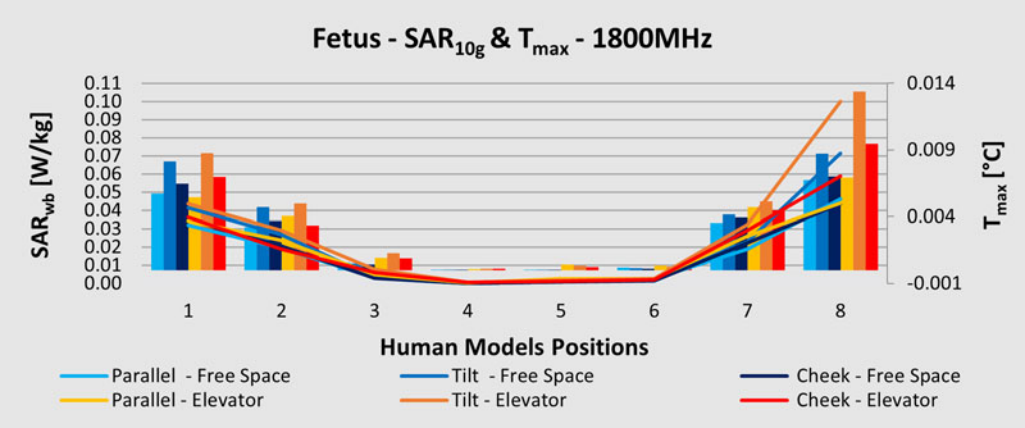

Fig. 19. Graphic representation of SAR-10 g [W/kg] and Tmax rise [°C] values in 7th month model fetus at 1800 MHz and for 1 W output power of the mobile phone. Eight human model positions (see Fig. 7) and three mobile phone positioning inside the elevator cabin and at free space are evaluated. SAR values are represented by the line distributions while the bars correspond to the temperature values.

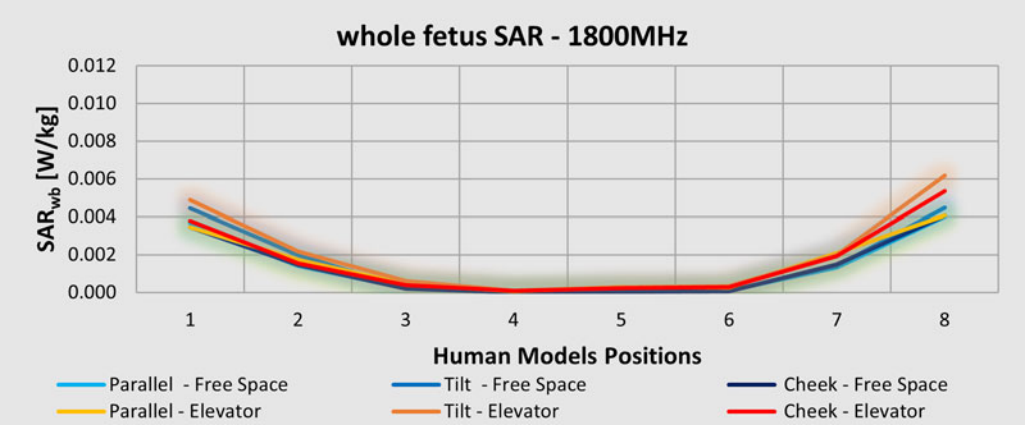

Fig. 20. Graphic representation of SAR whole-body (SARwb) [W/kg] in 7th month model fetus at 1800 MHz and for 1 W output power of the mobile phone. Eight human model positions (see Fig. 7) and three mobile phone positioning inside the elevator cabin and at free space are evaluated.

$SAR_{10\,g}$ value is 0.136 W/Kg at human position 2 at parallel phone position while inside the elevator cabin it is 0.165 W/Kg at human position 1 for the same phone position. Tilt phone position for all eight different configurations has higher values than the parallel and cheek positions. The $SAR_{10\,g}$ and T_{max} distributions at 1800 MHz inside the elevator cabin are similar to the corresponding ones at 1000 MHz. However, there is a notable increase in all the calculated values. They are almost doubled at 1800 MHz.

The graphic representation of the whole-body SAR for Pregnant woman at 1800 MHz is very similar with the one at 1000 MHz. The maximum values can be found at the tilt phone position inside the elevator cabin for all model configurations, while the minimum can be found at the cheek free space scenarios. The maximum SAR_{wb} value is 0.0291 W/Kg at free space and 0.0499 W/Kg, both at human position 3. The minimum SAR_{wb} value is 0.0186 and 0.00253 W/Kg at human position 1, cheek phone position at free space and inside the elevator cabin respectively.

The $SAR_{10\,g}$ along with the T_{max} for the operating mobile phone frequency of 1800 MHz of the 7th month fetus are presented in Fig. 19, while in Fig. 20 the whole-fetus SAR is presented. Fetus' $SAR_{10\,g}$ and T_{max} distributions at 1800 MHz are similar with the ones at 1000 MHz for all the simulating scenarios, but with moderately higher values for both the quantities. The maximum $SAR_{10\,g}$ value is 0.0714 and 0.1001 W/Kg at free space and inside the elevator cabin respectively. Both are calculated for human position 8 and tilt phone position. The next lower SAR10 g value is at tilt phone position 1 inside the elevator cabin. It is 28.6% lower. The minimum $SAR_{10\,g}$ value is 0.00009 W/Kg at human position 5 at cheek phone position at free space and 0.00029 W/Kg at human position 4 at parallel phone position inside the elevator cabin.

In contrast, the whole-fetus SAR (Fig. 20) has lower values as compared to those at 1000 MHz. The maximum SAR_{wb} value at 1800 MHz is found at human position 8 and tilt phone position. It is 0.0045 W/Kg at free space and 0.0068 W/Kg inside the elevator cabin. The minimum SAR_{wb} at free space is 0.00001 W/Kg at human position 5 at cheek phone position. It is 0.00006 W/Kg at human position 6 at parallel phone position inside the elevator cabin. Even though the SARwb values are very low, still there is a significant increase of the maximum values by about 51.11% inside the metallic cabin.

Discussion

Based on the obtained numerical results of SAR_{10g}, Roberta seems to be more affected by the mobile phone position than the human

https://doi.org/10.1017/S1759078722000253 Published online by Cambridge University Press

models' relevant positions for both frequencies. The phone positioning is the most important factor of variations for SAR_{10g}, SAR_{wb} and T_{max} of Roberta, and SAR_{wb} of Pregnant woman. The position of the phone is affecting in a smaller scale the values of SAR_{10g}, T_{max} of pregnant woman and fetus, and the whole fetus SAR. The positioning of the models is correlated with $SAR_{10\,g}$ and T_{max} of pregnant and fetus and whole fetus SAR, while it is not affecting Roberta's SAR values. Lastly, the metallic cabin elevator is generating larger values for all the human models, especially at SAR_{wb} levels.

At 1000 MHz, Roberta's $SAR_{10\,g}$ results are higher than 1800 MHz at tilt and cheek position, but lower at the parallel phone position. This is probably due to the different affected tissues since electromagnetic waves penetrate deeper at 1000 MHz than at 1800 MHz. More specifically, at 1800 MHz, the maximum values of both $SAR_{10\,g}$ and T_{max} were found at the ear skin tissue, at parallel and tilt phone configurations, and at skin tissue at the cheek. At 1000 MHz, the maximum values of both SAR and T_{max} were calculated at the ear cartilage tissue for parallel and tilt phone position, and at the muscle tissue for cheek position. Similarly, SAR_{wb} is affected both from the phone position and from the presence of the elevator cabin, especially at the frequency of 1000 MHz. In general, the SAR_{wb} of Roberta is higher inside the elevator cabin at 1000 MHz.

The temperature rise at Roberta model follows almost the same distribution as $SAR_{10\,g}$ measurements, but it is not directly proportional to the SAR distribution [9, 10]. At 1000 MHz the maximum temperature rise for the child model is at the cheek phone position at the 3rd model position and at free space. T_{max} at 1000 MHz at parallel phone position has an increase of 11.46% inside the elevator cabin, while at tilt phone position the increase is about 9.97% and at cheek phone position the T_{max} increase at the presence of metallic cabin is only 0.81% for Roberta model. Also, at 1800 MHz there is T_{max} increase of 0.21% inside the elevator at the parallel position, 27.58% at tilt position and 22.03% at cheek phone position. The maximum value of $T_{max,}$ at 1800 MHz, is at parallel phone position at the 6th model position and free space, differentiating from $SAR_{10\,g}$ maximum value which is found inside the elevator cabin at cheek phone position and at the 2nd relevant position of the human model. For all examined simulations, maximum temperature rise does not exceed 1°C.

For Pregnant woman most of the $SAR_{10\,g}$ values are higher at 1800 MHz operating frequency, while for the fetus most of the values are higher at 1000 MHz. This is expected since at the lower frequency the electromagnetic waves penetrate deeper and reach the fetus more easily [24–28]. Maximum SAR and T_{max} values on Pregnant II are all found at skin and muscle tissues, depending on both the positions of the models and the cell phone.

T_{max} for Pregnant II model at 1000 MHz inside the metallic cabin has an increase of 3.6% at parallel phone position, 1.3% at tilt and 4.35% at the cheek. At 1800 MHz the T_{max} values inside the elevator have an increase of 15.57% at parallel phone position, 1.53% at tilt and 10.69% at the cheek. SAR_{wb} for the pregnant woman even though it is generally low, inside the elevator cabin get a 100% increased at 1000 MHz and 66.67% at 1800 MHz which is a notable increase. In conclusion, the presence of the metallic elevator cabin has higher percentages at the maximum temperature values compared to free space.

Fetus maximum SAR and temperature rise values are found at positions where the mobile phone is in front of the pregnant abdomen and in the oblique direction of it, as in [30]. The maximum SAR and temperature rise values for the fetus are found at amniotic fluid due to the large electromagnetic conductivity and thermal capacity of the specific tissue. T_{max} values for fetus even though they are small, they have increased values inside the metallic cabin, for both 1000 and 1800 MHz. T_{max} values for the fetus at 1000 MHz increase inside the elevator about 28.57% at parallel phone position, 14.29% at tilt and 25% at cheek in comparison to free space. Notably, at 1800 MHz the increase of T_{max} values inside the elevator is approximately 0.95% at parallel phone position, 30.77% at tilt and 22.02% at the cheek. The larger calculated T_{max} is 0.18°C for pregnant and 0.014°C for the fetus. The difference is more profound than in [24] where Tmax in the fetus is less than half of the equivalent one in the pregnant woman. World Health Organization (WHO) [56], set the value of 1°C as the upper allowable limit. After EM experimentations on animals fetuses (mostly mice) higher temperature rise has been found to be causing health problems [56].

The values of maximum P_{abs} of the pregnant II are more than double of those of fetus, but the whole-body SAR and the whole fetus SAR are similar. The maximum P_{abs} for the pregnant woman is 0.335 W at tilt phone position, at the 6th relevant position of models and inside the elevator cabin while for fetus the maximum P_{abs} value is 0.0142 W at tilt phone position, at the 8th relevant position of the models and inside the metallic cabin. Therefore, it is believed that a dosimetry study of a pregnant woman, even if $SAR_{10\,g}$ is low for both pregnant and the fetus, it is equally important to consider the whole-body SAR.

All values of SAR are far below the permitted limits for $SAR_{10\,g}$ which is 2.0 W/kg and the temperature increase values are below the threshold temperature of 1°C for the time constant of 6 min (thermal time constant).

Conclusion

A detailed study of electromagnetic exposure and thermal safety, for a 5-year-old child and a 7th months pregnant woman, along with the fetus, inside a metallic elevator cabin is carried out. Numerically accurate anatomical human models and mobile phone model operating at two frequencies of 1000 and 1800 MHz are utilized. Totally 48 different configurations of the models are studied and analytical results of SAR_{10g}, SAR_{wb} and T_{max} are presented for all the human models and the fetus.

From the obtained results it appears that for a well-placed study, every quantity should be presented, and various configurations should be analyzed. Furthermore, the investigation in the elevator cabin, under different occupancy conditions and different operating mobile frequencies, should be explored.

References

1. **Zervos T, Alexandridis AA, Petrovic VV, Dangakis KP, Kolundzija BM, Djordjevic AR and Soras C** (2005) Mobile phone antenna performance and power absorption in terms of handset size and distance from user's head. *Wireless Personal Communications* **33**, 109–120.
2. **Kargel C** (2005) Infrared thermal imaging to measure local temperature rises caused by handheld mobile phones. *IEEE Transaction on Instrumentation and Measurement* **54**, 1513–1519.
3. **Ali MF and Ray S** (2009) SAR Analysis in a spherical inhomogeneous human head model exposed to radiating dipole antenna for 500 MHz–3 GHz using FDTD method. *International Journal of Microwave and Optical Technology* **4**, 35–40.
4. **Christopoulou M, Koulouridis S and Nikita KS** (2009) Parametric study of power absorption patterns induced in adult and child models by small helical antennas. *Progress In Electromagnetics Research, PIER* **94**, 49–67.

https://doi.org/10.1017/S1759078722000253 Published online by Cambridge University Press

5. **Mat DAA, Kho WT, Joseph A, Kipli K, Lias K, Marzuki ASW and Sahrani S** (2010) Electromagnetic radiation towards adult human head from handheld Mobile phones. *International Journal of Network and Mobile Technologies* **1**, 610–667.
6. **Sallomi AH** (2012) A theoretical approach for SAR calculation in human head exposed to RF signals. *Journal of Engineering and Development* **16**, 304–313.
7. **Al-Mously SI** (2011) Factors influencing the EM interaction between mobile phone antennas and human head. *Digital Information and Communication Technology and Its Applications*, Dijon, France.
8. **Razmadze A, Shoshiashvili L, Kakulia D and Zaridze R** (2009) Influence on averaging masses on correlation between mass-averaged SAR and temperature rise. *Journal of Applied Electromagnetism* **10**, 8–21.
9. **Sabbah AI, Dib NI and Al-Nimr MA** (2011) Evaluation of specific absorption rate and temperature elevation in a multi-layered human head model exposed to radio frequency radiation using the finite-difference time domain method. *IET Microwaves, Antennas & Propagation* **5**, 1073–1080.
10. **Sabbah AI, Dib NI and Al-Nimr MA** (2010) SAR And temperature evaluation In A multilayered human head model Due To An obliquely incident plane wave. *Progress in Electromagnetics Research M* **13**, 95–108.
11. **Wessapan T and Rattanadecho P** (2012) Numerical analysis of specific absorption rate and heat transfer in human head subjected to Mobile phone radiation: effects of user Age and radiated power. *Journal of Heat Transfer* **134**, 121101–121111.
12. **Wessapan T, Srisawatdhisukul S and Rattanadecho P** (2012) Specific absorption rate and temperature distributions in human head subjected to mobile phone radiation at different frequencies. *International Journal of Heat and Mass Transfer* **55**, 347–359.
13. **Hirata A and Shiozawa T** (2003) Correlation of maximum temperature increase and peak SAR in the human head due to handset antennas. *IEEE Trans. on Microwave Theory and Technique* **51**, 1834–1841.
14. **Hirata A, Fujimoto M, Asano T, Wang J, Fujiwara O and Shiozawa T** (2006) Correlation between maximum temperature increase and peak SAR with different average schemes and masses. *IEEE Transactions on Electromagnetic Compatibility* **48**, 569–578.
15. **Koulouridis S and Nikita KS** (2004) Study of the coupling between human head and cellular phone helical antennas. *IEEE Transactions on Electromagnetic Compatibility* **46**, 62–70.
16. **Beard BB, Kainz W, Onishi T, Iyama T, Watanabe S, Fujiwara O, Wang J, Bit-Babik G, Faraone A, Wiart J, Christ A, Kuster N, Lee A-K, Kroeze H, Siegbahn M, Keshvari J, Abrishamkar H, Simon W, Manteuffel D and Nikoloski N** (2006) Comparisons of computed Mobile phone induced SAR in the SAM phantom to that in anatomically correct models of the human head. *IEEE Transactions on Electromagnetic Compatibility* **48**, 397–407.
17. **Christ A, Gosselin M-C, Christopoulou M, Kuhn S and Kuster N** (2010) Age-dependent tissue-specific exposure of cell phone users. *Physics in Medicine & Biology* **55**, 1767–1783.
18. **Gosselin M-C, Christ A, Murbach M, Ryf S, Kühn S, Christopoulou M, Neufeld E, Gabriel C, Peyman A and Kuster N** (2008) Influences of age dependent tissue parameters and anatomical structures on SAR and temperature increase in the head of cellular phone users. *XXIX General Assembly of the International Union of Radio Science (URSI)*, Chicago, Illinois, USA.
19. **Fernandez-Rodriguez CE, De Salles AAA and Davis DL** (2015) Dosimetric simulations of brain absorption of mobile phone radiation – the relationship between psSAR and age. *IEEE Access* **3**, 2425–2430.
20. **Lu M and Ueno S** (2012) Comparison of specific absorption rate induced in brain tissues of a child and an adult using mobile phone. *Journal of Applied Physics* **111**, 07B311–07B313.
21. **Wiart J, Hadjem A, Wong MF and Bloch I** (2008) Analysis of RF exposure in the head tissues of children and adults. *Physics in Medicine & Biology* **53**, 3681–3695.
22. **Gandhi OP** (2015) Yes the children are more exposed to radiofrequency energy from mobile telephones than adults. *IEEE Access* **3**, 985–988.
23. **Morris RD, Lloyd Morgan L and Davis D** (2015) Children absorb higher doses of radio frequency electromagnetic radiation from mobile phones than adults. *IEEE Access* **3**, 2379–2387.
24. **Takei R, Nagaoka T, Nishino K, Saito K, Watanabe S and Takahashi M** (2018) Specific absorption rate and temperature increase in pregnant women at 13, 18, and 26 weeks of gestation due to electromagnetic wave radiation from a smartphone. *IEICE Communications Express* **7**, 212–217.
25. **Togashi T, Nagaoka T, Kikuchi S, Saito K, Watanabe S, Takahashi M and Ito K** (2008) FDTD calculations of specific absorption rate in Fetus caused by electromagnetic waves from Mobile radio terminal using pregnant woman model. *IEEE Transactions on Microwave Theory and Techniques* **56**, 554–559.
26. **Akimoto S, Kikuchi S, Nagaoka T, Saito K, Watanabe S, Takahashi M and Ito K** (2010) Evaluation of specific absorption rate for a fetus by portable radio terminal close to the abdomen of a pregnant woman. *IEEE Transactions On Microwave Theory and Techniques* **58**, 3859–3865.
27. **Hand JW, Li Y, Thomas EL, Rutherford MA and Hajnal JV** (2006) Prediction of specific absorption rate in mother and Fetus associated With MRI examinations during pregnancy. *Magnetic Resonance in Medicine* **55**, 883–893.
28. **Chiaramello E, Parazzini M, Fiocchi S, Ravazzani P and Wiart J** (2017) Assessment of fetal exposure to 4 G LTE tablet in realistic scenarios: effect of position, gestational age, and frequency. *IEEE Journal of Electromagnetics, RF and Microwaves in Medicine and Biology* **1**, 26–33.
29. **Fiocchi S, Markakis IA, Ravazzani P and Samaras T** (2013) SAR Exposure from UHFRFID reader in adult, child, pregnant woman, and fetus anatomical models. *Bioelectromagnetics* **34**, 443–452.
30. **Fiocchi S, Parazzini M, Liorni I, Samaras T and Ravazzani P** (2014) Temperature increase in the fetus exposed to UHF RFID readers. *IEEE Transactions On Biomedical Engineering* **61**, 2011–2019.
31. **Nagaoka T, Saito K, Takahashi M, iIto K and Watanabe S** (2008) Estimating specific absorption rates in pregnant women by using models at 12-, 20–, and 26-weeks' gestation for plane wave exposures. *International Symposium on Electromagnetic Compatibility – EMC Europe*, Hamburg, Germany.
32. **Nagaoka T, Saito K, Takahashi M, Ito K and Watanabe S** (2008) Anatomically realistic reference models of pregnant women for gestation ages of 13, 18, and 26 week. *International Conference of the IEEE Engineering in Medicine and Biology Society (EMBS)*, Vancouver, BC, Canada.
33. **Leung S-W, Diao Y, Chan K-H, Siu Y-M and Wu Y** (2012) Specific absorption rate evaluation for passengers using wireless communication devices inside vehicles With different handedness, passenger counts, and seating locations. *IEEE Transactions on Bio-medical Engineering* **59**, 2905–2912.
34. **Tang CK, Fung LC and Leung SW** (2007) Electromagnetic field radiation of mobile phone inside metallic enclosure. *IEEE International Symposium on Electromagnetic Compatibility*, Honolulu, HI, USA, 9–13 July 2007.
35. **Ruddle AR** (2007) Computed SAR distributions for the occupants of a car with a 400 MHz transmitter on the rear seat. *18th International Zurich Symposium on Electromagnetic Compatibility*, Munich, Germany.
36. **Lazarescu C, David V, Nica I and Dafinescu V** (2012) Walls effect over the specific absorbtion rate in the human head due to mobile phone exposure. *International Conference and Exposition on Electrical and Power Engineering (EPE 2012)*, Iasi, Romania.
37. **Jemima Priyadarshini S, Anita Jones Mary T, Sugumar D and Ravichandran CS** (2010) Impact of SAR on human head modeling in elevators using IFA. *IEEE Asia-Pacific Conference on Applied Electromagnetics (APACE)*, Port Dickson, Malaysia.
38. **Tang CK, Chan KH, Fung LC and Leung SW** (2008) Effect on radio frequency human exposure of mobile phone inside an enclosed metallic elevator. *Microwave and Optical Technology Letters* **50**, 2207–2210.
39. **Tang CK, Chan KH, Fung LC and Leung SW** (2008) Antenna performance of mobile phone and corresponding human exposure inside fully and partially enclosed metallic elevator. *IEEE International Symposium on Electromagnetic Compatibility*, Detroit, USA.
40. **Simba AY, Hikage T, Watanabe S and Nojima T** (2009) Specific absorption rates of anatomically realistic human models exposed to RF electromagnetic fields from Mobile phones used in elevators. *IEEE Transactions on Microwave Theory and Techniques* **57**, 1250–1259.
41. **Karatsi I and Koulouridis S** (2014) E-field distribution and dosimetry of an anatomical human body model, inside elevator cabin: Comparison

https://doi.org/10.1017/S1759078722000253 Published online by Cambridge University Press

between five different structures of elevator cabins. *4th International Conference on Wireless Mobile Communication and Healthcare - Transforming Healthcare Through Innovations in Mobile and Wireless Technologies (MOBIHEALTH)*, Athens, Greece.
42. **Chan KH, Leung SW and Siu YM** (2010) Specific absorption rate evaluation for people using wireless communication device in vehicle. *IEEE International Symposium on Electromagnetic Compatibility (EMC)*, Fort Lauderdale, FL, USA.
43. **Chen G, Deng J and Yi J** (2014) A software frame of elevator signal amplifier network with self-diagnosis. *IEEE 13th International Conference on Cognitive Informatics and Cognitive Computing*, London, UK.
44. **Pinto YC, Ghanmi A, Hadjem A, Conil E, Namur T, Person C and Wiart J** (2011) Numerical Mobile phone models validated by SAR measurements, Eucap, Rome, April 2011.
45. IEEE/IEC 62209-1528-2020 - IEC/IEEE International Standard - Measurement procedure for the assessment of specific absorption rate of human exposure to radio frequency fields from hand-held and body-mounted wireless communication devices – Part 1528: Human models, instrumentation, and procedures (Frequency range of 4 MHz to 10 GHz), 19 October 2020.
46. CENELEC Human exposure to radio frequency fields from hand-held and body-mounted wireless communication devices. Human models, instrumentation, and procedures. Part 2: Procedure to determine the specific absorption rate (SAR) for wireless communication devices used. CENELEC EN62209-2-2010.
47. Schmid & Partner Engineering AG: http://www.speag.com/speag.
48. IEEE C95.1-2019/Cor 2-2020 - IEEE Standard for Safety Levels with Respect to Human Exposure to Electric, Magnetic, and Electromagnetic Fields, 0 Hz to 300 GHz - Corrigenda 2, 2019–2020.
49. **ICNIRP** (2020) Guidelines for limiting exposure to, electromagnetic fields (100KHz to 300 GHz). ICNIRP Guidelines.
50. **Pennes HH** (1948) Analysis of tissue and arterial blood temperatures in resting forearm. *Journal of Applied Physiology* **1**, 93–122.
51. **Christ A, Guldimann R, Buhlmann B, Zefferer M, Bakker JF, Van Rhoon GC and Kuster N** (2012) Exposure of the human body to professional and domestic induction cooktops compared to the basic restrictions. *Bioelectromagnetics* **33**, 695–705.
52. **Bakker JF, Paulides MM, Neufeld E, Christ A, Kuster N and van Rhoon GC** (2011) Children and adults exposed to electromagnetic fields at the ICNIRP reference levels: theoretical assessment of the induced peak temperature increase. *Physics in Medicine & Biology* **56**, 4967–4989.
53. **Gosselin M-C, Neufeld E, Moser H, Huber E, Farcito S, Gerber L, Jedensjö M, Hilber I, Di Gennaro F, Lloyd B, Cherubini E, Szczerba D, Kainz W and Kuster N** (2014) Development of a New generation of high-resolution anatomical models for medical device evaluation: the virtual population 3.0. *Physics in Medicine and Biology* **59**, 5287–5303.
54. Greece New Building Regulations, Law 4067/12 GG – 79, A/12.
55. The Hellenic Accreditation System (ESYD), KO-ANEL 01/04/16-1-2014.
56. **WHO** (1993) Environmental health criteria 137: Electromagnetic fields (300 kHz to 300 GHz). Geneva, Switzerland.

Ioanna Karatsi obtained a master's degree diploma in mechanical engineering from the Department of Mechanical and Aeronautical Engineering, School of Engineering, University of Patras, in 2010. She is a Ph.D. student in the Department of Electrical and Computer Engineering at the University of Patras. She has authored conference papers, participated, and has been a member of the organizing committee and supported international conferences. Her research interests are electromagnetic radiation and protection and ergonomics.

Sofia Bakogianni obtained a diploma degree in electrical and computer engineering from the National Technical University of Athens, Athens, Greece, in 2007, an M.Sc. in microelectronics-optoelectronics from the University of Crete, Heraklion, Greece, in 2010, and a Ph.D. in electrical and computer science from the University of Patras, Patras, Greece, in 2018. She has authored or coauthored more than 15 journal and conference papers. Her current research interests include bioelectromagnetics, wearable/implantable antennas, and antenna theory. Dr. Bakogianni is a member of the Technical Chamber of Greece. She was a recipient of National Awards and Scholarships. She is a reviewer of the *IEEE Transactions on Antennas and Propagation, IEEE Antennas and Wireless Propagation Letters*, and of various international conferences.

Stavros Koulouridis obtained a diploma degree in electrical and computer engineering and a Ph.D. in microwave engineering from National Technical University of Athens, Greece, in 1999 and 2003, respectively. From 2004 to 2008, he worked as a postdoctoral researcher with the Electroscience Laboratory, The Ohio State University, Columbus, OH, USA. He joined the Electrical and Computer Engineering Department, University of Patras, Greece, in March 2009. Since March 2020, he has been an associate professor and from October 2020, he has been the Director of the RF, Microwave and Mobile Communications Laboratory. His research interests include antenna and microwave devices design, development and fabrication of novel materials, microwave applications in medicine, and electromagnetic optimization techniques. He was the general chair of the International Workshop in Antennas Technology (IWAT) 2017. From 2010 he has been serving in the Technical Program Committee for IEEE Antennas and Propagation Society (AP-S) International Symposium. Since 2015, he has been serving in the Technical Program Committee of European Conference of Antennas and Propagation (EUCAP) as a meta-reviewer. He is a topical advisory panel member of Electronics and Editorial Board Member of Telecom, Open Access Journals from MDPI. He is an associate editor of IEEE AWPL and IEEE J-ERM.

https://doi.org/10.1017/S1759078722000253 Published online by Cambridge University Press